

First Demonstration of a MEMS Tunable Vertical-Cavity SOA

Qi Chen, Garrett D. Cole, E. Staffan Björilin, *Member, IEEE*, Toshio Kimura, Shaomin Wu, Chad S. Wang, *Student Member, IEEE*, Noel C. MacDonald, *Fellow, IEEE*, and John E. Bowers, *Fellow, IEEE*

Abstract—We present the first microelectromechanical tunable vertical-cavity semiconductor optical amplifier. The device operates in the long wavelength range and exhibits a minimum of 10 dB of device gain through 11 nm of tuning.

Index Terms—Laser amplifiers, microelectromechanical (MEMS) devices, optical pumping, semiconductor optical amplifiers (SOAs), surface-emitting lasers, tunable amplifiers.

I. INTRODUCTION

LONG-WAVELENGTH vertical-cavity semiconductor optical amplifiers (VCISOAs) are attractive as a low-cost alternative to erbium-doped fiber amplifiers and conventional in-plane SOAs for applications in metro-area networks and fiber to the home. Due to the vertical-cavity geometry, VCISOAs enjoy benefits such as high fiber coupling efficiency, polarization-independent gain, the potential to fabricate two-dimensional arrays, and the ability to test devices on wafer. In recent years, both optically and electrically pumped long-wavelength VCISOAs have been demonstrated [1]–[4].

As shown previously, the high finesse Fabry–Pérot (FP) cavity of fixed wavelength VCISOAs results in a narrow gain bandwidth [1]. This inherent filtering effect is advantageous for preamplifier applications as it eliminates out-of-band noise and provides channel selection in multiwavelength systems [2]. In order to make VCISOAs more flexible for such applications, tunable devices must be developed. Previously, temperature tuning of long wavelength VCISOAs has been investigated [4], but a more promising method is microelectromechanical (MEMS) tuning. In this case, mechanical alteration of the effective FP mode gives rise to tuning ranges greater than those that can be achieved by refractive index modulation.

The use of MEMS tuning is a popular mechanism for wavelength selection in vertical-cavity devices, including vertical-cavity surface-emitting lasers [5]–[7], resonant-cavity light-emitting diodes [8], asymmetric FP modulators [9], and

Manuscript received January 5, 2004; revised March 1, 2004. This work was supported in part by the Defense Advanced Research Projects Agency (DARPA) through the Center for Chips with Heterogeneously Integrated Photonics (CHIPS) and NSF IGERT Advanced Optical Materials (AOM) Program under Award DGE-9987618.

Q. Chen, E. S. Björilin, T. Kimura, S. Wu, C. S. Wang, and J. E. Bowers are with the Electrical and Computer Engineering Department, University of California Santa Barbara, Santa Barbara, CA 93106 USA.

G. D. Cole and N. C. MacDonald are with the Materials Department, University of California Santa Barbara, Santa Barbara, CA 93106 USA (e-mail: gcole@engineering.ucsb.edu).

Digital Object Identifier 10.1109/LPT.2004.827428

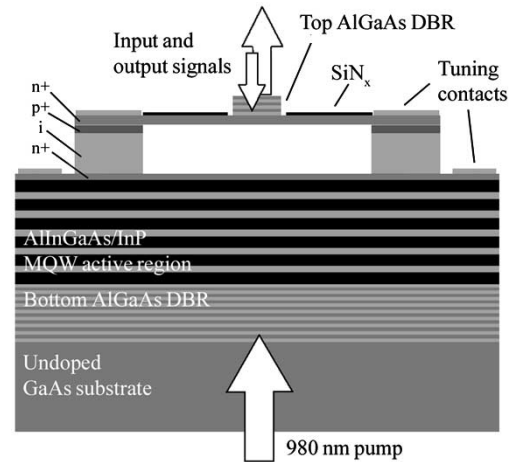


Fig. 1. Cross-sectional schematic of the MT-VCISOA structure.

vertical-cavity filters [10]. In this letter, we present the first MEMS tunable VCISOA (MT-VCISOA).

II. DEVICE DESIGN AND FABRICATION

A. Device Structure

Fig. 1 shows a schematic of the MT-VCISOA. The device utilizes an InP-based active region bonded to two AlGaAs distributed Bragg reflectors (DBRs). The active region contains five sets of five compressively strained AlInGaAs quantum wells (QWs) placed at the peaks of the standing optical wave in a $5/2\text{-}\lambda$ cavity. The peak gain of the active region is designed to be at 1545 nm at room temperature. The bottom mirror is a 30-period GaAs–Al_{0.98}Ga_{0.02}As DBR with a calculated reflectivity of 0.999. The top DBR consists of four periods of GaAs–Al_{0.98}Ga_{0.02}As on top of a $3/4\text{-}\lambda$ n⁺ GaAs layer, a $5/4\text{-}\lambda$ (optical thickness in air) Al_{0.98}Ga_{0.02}As sacrificial etch layer, and a $1/4\text{-}\lambda$ n⁺ GaAs layer directly above the active region. This structure forms a 5.5-period DBR including the air gap as a low index layer. The peak reflectivity of the top DBR is calculated to be 0.976. The MT-VCISOA is designed to be pumped optically, and to operate in reflection mode.

As shown in the schematic, the GaAs membrane and the $1/4\text{-}\lambda$ GaAs layer closest to the active region are doped n⁺. The sacrificial layer is comprised of 200 nm of p⁺Al_{0.98}Ga_{0.02}As, followed by 1750 nm of intrinsic Al_{0.98}Ga_{0.02}As. A reverse bias across this n⁺-p⁺-i-n⁺ diode creates an electrostatic force that displaces the membrane toward the substrate, reducing the air-gap thickness and phase shifting the upper DBR. The diode is designed to have a reverse breakdown voltage of 60 V.

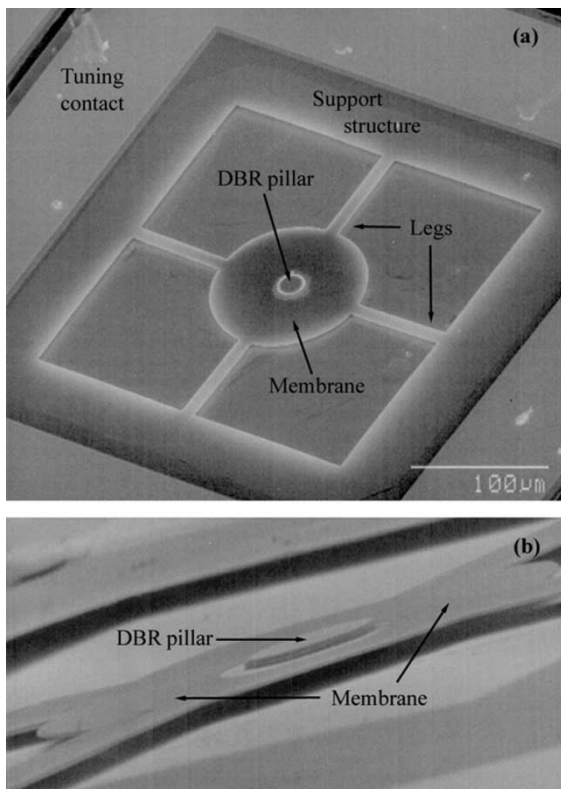


Fig. 2. SEM images of a MT-VCSOA structure showing (a) an overview of the device, and (b) a close-up of the released top membrane.

B. Device Fabrication

Initially, both the InP-based active region and the membrane DBR structure are transferred to a GaAs substrate containing the 30-period bottom mirror using direct wafer bonding [11]. Following this step, the uppermost four-period DBR pillar is defined using a SiCl_4 reactive ion etch. Electrical contacts are formed on the n^+ GaAs layers by electron beam evaporation of Ge–Au–Ni–Au. Before release, a thin layer of tensile-stressed (260 MPa) SiN_x is deposited on top of the membrane and legs. This film creates a slight tensile stress in the structure to ensure the flatness of the free-standing membrane. To create the air gap, the sacrificial $\text{Al}_{0.98}\text{Ga}_{0.02}\text{As}$ layer is selectively wet-etched with a dilute HCl solution. As a result of the undercut etch, the p^+ $\text{Al}_{0.98}\text{Ga}_{0.02}\text{As}$ layer directly below the GaAs membrane is removed from the optical cavity. This procedure eliminates the need for light to travel through highly p-doped material, thereby minimizing absorption loss. In the final step, a CO_2 critical point drying system is used to avoid stiction of the released membrane. A scanning electron micrograph (SEM) of a finished device is shown in Fig. 2.

III. EXPERIMENTAL SETUP AND RESULTS

For our experimental setup, an external cavity tunable laser diode is used as a signal source, while the input signal power is controlled by a variable optical attenuator to be -35 dBm. In all tests, the amplifier is operated below saturation. The signal is coupled into and out of the top of the device through a fiber focuser. A circulator is used to separate the two signals and we use an optical spectrum analyzer to monitor the output signal. A

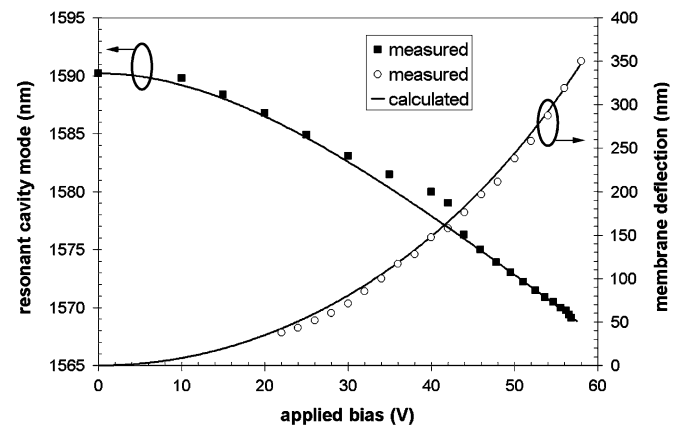


Fig. 3. Resonance wavelength and membrane deflection versus tuning bias.

980-nm laser, which is coupled in through the bottom DBR by another fiber focuser, serves as the optical pump. The coupling loss through the setup is measured to be about 7 dB.

Following processing, the air-gap thickness is measured using a white light interferometer. In this case, the devices show a much larger air gap than the ideal $5/4\lambda$ design of 1950 nm. The actual air-gap thickness measured for the device presented here is 3911 nm, due to stress-related deformation of the undercut support structure. The dynamic displacement of the released membrane is measured using a laser Doppler vibrometer. As shown in Fig. 3, the membrane is displaced by 340 nm with a reverse bias of 57 V. In this device, the increase in the air-gap thickness caused by the support deflection greatly diminishes the applied force. With the ideal air gap, the bias required for 340 nm of displacement would be reduced to 25 V. As expected, the deflection shows a parabolic dependence with the applied voltage and the experimental data matches well with the values generated by a one-dimensional electromechanical model similar to that described in [12].

Using the measured deflection data, the resonance wavelength of the device can be calculated. As shown in Fig. 3, the resonant cavity mode blue-shifts from 1590 to 1569 nm with a total membrane displacement of 340 nm (tuning bias of 57 V). The measured resonance wavelength follows the theoretical values extremely well; the points of largest error exhibit a red-shift in wavelength due to heating from the high pump power, which is not taken into account in the model.

Fig. 4 presents the pump power required for 10-dB device gain (3-dB fiber-to-fiber), as well as the calculated mirror reflectance, versus wavelength. The reflectance data is generated using an optical simulation program (VERTICAL), while the required pump power is estimated by combining the reflection mode FP gain equation with the carrier rate equation assuming below saturation conditions. As shown in the plot, the MT-VCSOA must be tuned from 1590 to 1580 nm before 10 dB of device gain is observed. Device gain larger than 10 dB is measured for wavelengths between 1580 and 1569 nm, yielding a tuning range of 11 nm. A maximum device gain of 17 dB is measured at 1570 nm. As the cavity mode is tuned closer to the QW gain peak less pump power is needed to reach the same gain. In this case, the rolloff in material gain at longer wavelengths necessitates higher pump power to achieve the

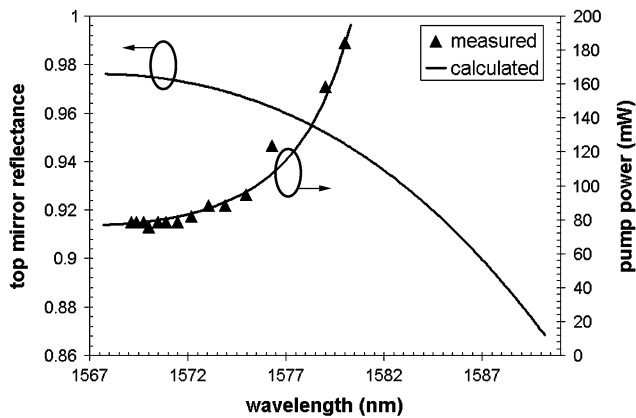


Fig. 4. Calculated top mirror reflectance and optical pump power required for 10-dB device gain versus wavelength.

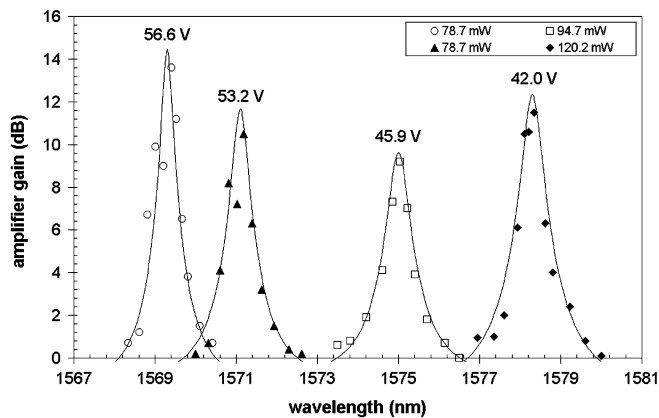


Fig. 5. Amplifier gain spectrum at multiple tuning bias values. The required pump power for each data set is included in the legend.

same gain value. In addition to the gain rolloff, the increase in pump power at longer wavelengths is also attributed to insufficient top mirror reflectance.

Over the tuning range, the calculated top DBR reflectance varies from 86.8% at the initial cavity mode to 97.6% near the breakdown voltage of the diode (measured to be 57 V). Because of the nonideal membrane deflection, the initial air gap results in an optical thickness near a multiple of $1/2\lambda$. At this point, the reflection from the first air–semiconductor interface and the reflection from the bottom of the membrane are nearly out of phase. As the device is tuned, the decreasing air-gap thickness begins to approach an odd multiple of $1/4\lambda$, and the reflected waves begin to add in phase, leading to a large increase in reflectance of the top mirror structure.

Fig. 5 shows the MT-VCSSOA gain spectrum at various tuning voltages and pump powers, with an input signal strength of -35 dBm. The solid lines are calculated curve fits based on the FP equations, as described in [1] and [4]. As the device is tuned to shorter wavelengths, the optical bandwidth decreases, even with the lower pump power shown. This decrease in bandwidth

is due to the increased top mirror reflectance at higher tuning bias values. Conversely, at longer wavelengths the reduced top mirror reflectance results in a broadening of the amplifier gain spectrum.

IV. CONCLUSION

An MT-VCSSOA has been fabricated using GaAs-InP wafer bonding and GaAs-based micromachining techniques. The device shows a minimum of 10-dB device gain over 11 nm of tuning, with a peak amplifier gain of 17 dB at 1570 nm. With an ideal air gap of $5/4\lambda$, the device should be capable of tuning ranges greater than 20 nm, centered at the peak reflectivity of the top DBR structure. In addition, the reduced air-gap thickness would allow for much lower tuning voltages. As demonstrated, MT-VCSSOAs may be attractive for applications as tunable preamplifiers and tunable receivers.

REFERENCES

- [1] J. Piprek, E. S. Björilin, and J. E. Bowers, "Optical gain-bandwidth product of vertical cavity laser amplifiers," *Electron. Lett.*, vol. 37, pp. 289–299, Mar. 2001.
- [2] E. S. Björilin, J. Geske, and J. E. Bowers, "Optically preamplified receiver at 10 Gb/s using a vertical cavity SOA," *Electron. Lett.*, vol. 37, pp. 1474–1475, Nov. 2001.
- [3] R. Lewen, K. Streubel, A. Karlsson, and S. Rapp, "Experimental demonstration of a multifunctional long-wavelength vertical-cavity laser amplifier-detector," *IEEE Photon. Technol. Lett.*, vol. 10, pp. 1067–1069, Aug. 1998.
- [4] T. Kimura, E. S. Björilin, J. Piprek, and J. E. Bowers, "High-temperature characteristics and tunability of long-wavelength vertical-cavity semiconductor optical amplifiers," *IEEE Photon. Technol. Lett.*, vol. 15, pp. 1501–1503, Nov. 2003.
- [5] M. S. Wu, E. C. Vail, G. S. Li, W. Yuen, and C. J. Chang-Hasnain, "Tunable micromachined vertical cavity surface emitting laser," *Electron. Lett.*, vol. 31, pp. 1671–1672, Sept. 1995.
- [6] M. C. Larson, A. R. Massengale, and J. S. Harris Jr., "Continuously tunable micromachined vertical-cavity surface-emitting laser with 18 nm wavelength range," *Electron. Lett.*, vol. 32, pp. 330–332, Feb. 1996.
- [7] P. Tayebati, P. D. Wang, D. Vakhshoori, C. C. Lu, M. Azimi, and R. N. Sacks, "Half-symmetric cavity tunable microelectromechanical VCSEL with single spatial mode," *IEEE Photon. Technol. Lett.*, vol. 10, pp. 1679–1681, Dec. 1998.
- [8] G. L. Christensen, A. T. T. D. Tran, Z. H. Zhu, Y. H. Lo, M. Hong, J. P. Mannaerts, and R. Bhat, "Long-wavelength resonant vertical-cavity LED/photodetector with a 75-nm tuning range," *IEEE Photon. Technol. Lett.*, vol. 9, pp. 725–727, June 1997.
- [9] W. S. Rabinovich, T. H. Stievater, N. A. Papanicolaou, D. S. Katzer, and P. G. Goetz, "Demonstration of a microelectromechanical tunable asymmetric Fabry–Pérot quantum well modulator," *Appl. Phys. Lett.*, vol. 83, no. 10, pp. 1923–1925, Sept. 2003.
- [10] J. Daleiden, N. Chitica, M. Strassner, A. Spisser, J. L. Leclercq, P. Viktorovitch, D. Rondi, E. Goutain, J. Peerlings, J. Pfeiffer, R. Reimenschneider, and K. Hjort, "Tunable InP/air gap Fabry–Pérot filter for wavelength division multiplex fiber optical transmission," in *Proc. 11th Int. Conf. InP and Related Materials*, May, 16–20 1999, Paper TuA3-4, pp. 285–287.
- [11] A. Black, A. R. Hawkins, N. M. Margalit, D. I. Babić, A. L. Holmes Jr., Y.-L. Chang, P. Abraham, J. E. Bowers, and E. L. Hu, "Wafer fusion: Materials issues and device results," *IEEE J. Select. Topics Quantum Electron.*, vol. 3, pp. 943–951, June 1997.
- [12] M. C. Larson, "Microelectromechanical wavelength-tunable vertical-cavity light emitters and lasers," Ph.D. dissertation, Stanford University, Stanford, CA, 1996.